Bray, J. D. "Developing Mitigation Measures for the Hazards Associated with Earthquake Surface Fault Rupture," in A Workshop on *Seismic Fault-Induced Failures – Possible Remedies for Damage to Urban Facilities*, Research Project 2000 Grant-in-Aid for Scientific Research (No. 12355020), Japan Society for the Promotion of Science, Workshop Leader, Kazuo Konagai, University of Tokyo, Japan, pp. 55-79, January 11-12, 2001 [Invited Paper].

DEVELOPING MITIGATION MEASURES FOR THE HAZARDS ASSOCIATED WITH EARTHQUAKE SURFACE FAULT RUPTURE

Jonathan D. Bray

Ph.D., P.E., Professor, Dept. of Civil and Environmental Eng., University of California, Berkeley
(440 Davis Hall, MC-1710, Berkeley, CA 94720-1710, USA, bray@ce.berkeley.edu)

Recent earthquakes have reminded the profession of the devastating effects of earthquake surface fault rupture on engineered structures and facilities. Insights from these events are discussed with special emphasis on describing how ground movements associated with surface faulting affect structures. Analytical procedures that can be employed to evaluate the hazards associated with surface faulting and to develop reasonable mitigation measures are also discussed. A project in Southern California where these procedures were applied is presented to illustrate the insight gained from sound engineering analysis of the problem. Similar to other forms of ground failure, such as mining subsidence, landslides, and lateral spreading, effective design strategies can be employed to address the hazards associated with surface faulting. These design measures include establishing non-arbitrary setbacks based on fault geometry, fault displacement, and the overlying soil; constructing earth fills, often reinforced with geosynthetics, to partially absorb underlying ground movements; using slip layers to decouple ground movements from foundation elements; and designing strong, ductile foundation elements that can accommodate some level of deformation without compromising the functionality of the structure.

Key Words: *earthquake engineering, earthquake fault rupture, ground movement, mitigation, design, surface faulting hazard, fault displacement, foundation engineering, compacted fill*

1. INTRODUCTION

Recent earthquakes have provided numerous examples of the devastating effects of earthquake surface fault rupture on the built environment. Surface fault rupture along the Chelungpu fault during the 1999 Chi-Chi, Taiwan earthquake ripped apart buildings, thrust buildings laterally, and racked buildings due to differential vertical ground movements. Similarly, surface ruptures displaced bridges, buildings, and buried lifelines during the 1999 Kocaeli and Duzce earthquakes in Turkey. Although less damaging due to the sparseness of facilities in the California Desert, the 1992 Landers earthquake produced broad zones of ground ruptures along 80 km of five distinct fault traces, which impacted buildings and lifelines traversing and adjacent to them.

Along with the often-spectacular observations of damage documented by these recent events, examples of satisfactory performance of structures emerged. Some facilities were sufficiently strong to withstand the underlying fault-induced ground movements without collapse. Other buildings were sufficiently ductile to deform in response to the tectonic ground displacements without failing. Other buildings were somewhat isolated from the majority of differential ground displacement, such that the building underwent some rigid body translation and rotation, without undergoing the internal deformation that is so damaging to a structure. These examples of satisfactory performance provide motivation for the notion that similar to other forms of ground failure effective design strategies can be developed to address the hazards associated with earthquake surface fault rupture.

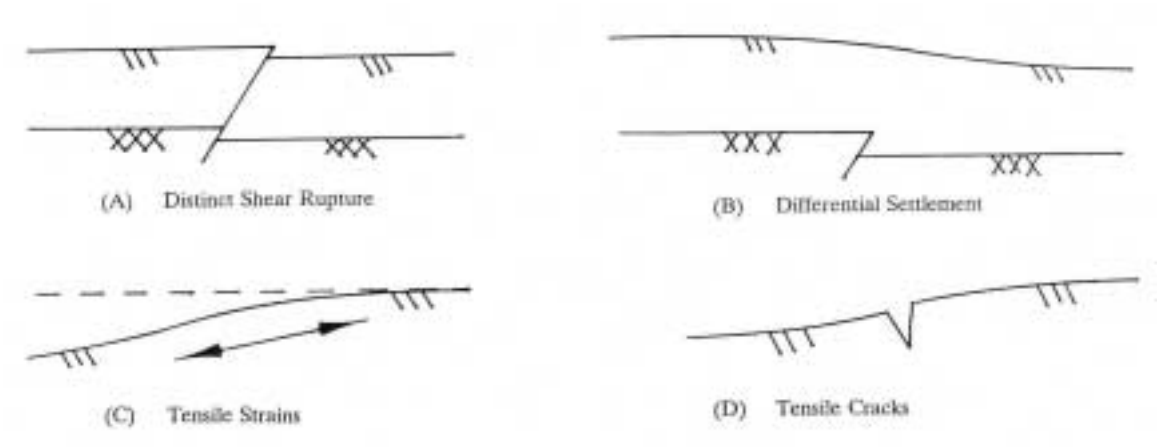

Figure 1 Principal surficial hazards of earthquake fault rupture.

2. HAZARDS ASSOCIATED WITH SURFACE FAULTING

2.1 Earthquake fault rupture

The principal factors controlling the general characteristics of surface faulting are: (a) the type of fault movement (reverse, normal, or strike-slip), (b) the inclination of the fault plane, (c) the amount of displacement on the fault, (d) the depth and geometry of the earth materials overlying the bedrock fault, (d) the nature of the overlying earth materials, and (e) the definition of the fault (i.e. well-established or more recently developed). Typically (Bray et al. 1994a), reverse faults tend to gradually decrease in dip near the ground surface. Normal faults tend to refract at the soil-bedrock contact and increase in dip as they approach the ground surface. This refraction and variation of the dip of the normal fault plane may produce gravity grabens. Strike-slip faults tend to follow the almost vertical orientation of the underlying bedrock fault, although the rupture zone may spread or "flower" near the ground surface. Relative motion is primarily concentrated within a relatively narrow zone above the bedrock fault. Once failure occurs, differential movement is usually localized to thin, distinct failure planes. Ductile materials, however, may accommodate significant fault movement by warping without actually developing distinct shear surfaces.

2.2 Hazards

The principal surficial hazards of base rock fault displacements are (**Fig. 1**):

(A) propagation of the distinct shear rupture plane to the ground surface,
(B) differential settlement or angular distortion of the ground surface,
(C) compressive or tensile horizontal strains at the ground surface, and
(D) development of surficial tension cracks.

The potential development of surficial tension cracks (Hazard D) can be evaluated by examining the other three hazards. Hence, this paper focuses on Hazards A-C. It is recognized that Hazard A constitutes the potentially most damaging hazard, and that in cases where Hazard A is unlikely, Hazards B and C will govern design recommendations regarding the surface fault rupture hazard. Of course, the earthquake event that produces the relative movement on surface fault features will also produce strong ground shaking. This paper focuses on the response of the overlying earth materials and built structures to base rock fault displacements and does not address the potential for building damage due to earthquake strong ground shaking, which could be especially severe in the near-fault region.

2.3 Mitigation basis

A number of previous studies (e.g. Bonilla 1970, Cole & Lade 1984, Bonilla 1988, Bray 1990, Bray et al. 1992, Bray et al. 1993a, Bray et al. 1993b, Lazarte et al. 1994, Bray et al. 1994a, Bray et al. 1994b, Lazarte & Bray 1995, and Lazarte & Bray 1996) indicate that the differential movement across an underlying distinct bedrock fault dissipates as the shear rupture plane propagates through previously unfractured overlying soils. If the depth of soil is sufficiently large, the soil response is sufficiently ductile, and the underlying fault displacement is sufficiently small, the differential displacement of the underlying fault can be "locally absorbed" within the overlying soil. In these cases, a distinct surface rupture does not reach the ground surface; instead, the base movement is “spread out” over a wider zone.

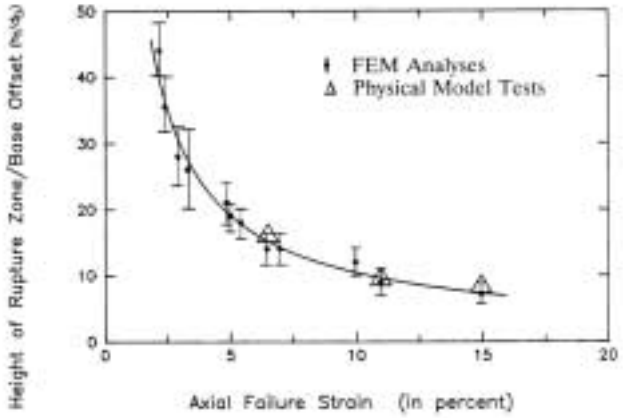

Figure 2 Normalized height of shear rupture zone in soil overlying base rock fault as a function of soil's failure strain (after Bray et al. 1994b).

The distance that a distinct bedrock rupture propagates up through overlying earth materials that were previously unfractured is primarily a function of the ductility of the overlying materials and the amount of relative displacement across the bedrock fault. Numerical simulations validated by the results of carefully performed physical model experiments and the trends found in documented field studies indicate that at a specified amount of bedrock fault displacement, the height that the shear rupture will propagate up into the overlying soil can be related to the failure strain of the soil as shown in **Figure 2** (Bray et al. 1994b). These data suggest that analytical procedures may be used to evaluate the consequences of surface fault rupture and to develop mitigation measures.

Using these approaches, the angular distortion and tensile ground strains developed at the ground surface can be used to evaluate fault setback criteria when the ground deformation is significant and to evaluate mitigation measures when the level of ground deformation can be made to be tolerable. As the ductility of the soil that overlies the bedrock fault has been found to be an important soil response characteristic, fill-reinforcement materials can be used to optimize the depth of over-excavation and fill replacement that would be necessary to mitigate the surficial hazards of earthquake fault rupture at a project site (Bray et al. 1993a).

3. RECENT OBSERVATIONS OF SURFACE FAULT RUPTURE

3.1 General

Comprehensive summaries of some of the principal observations of surface fault rupture may be found in papers such as Bonilla (1970), Sherard et al. (1974), and Bray et al. (1994a). Observations documented in these and other pertinent papers are not repeated in this paper, so the reader is asked to refer to these papers for a discussion of events occurring previous to the most recent events. In this paper, some key observations from important surface rupture events that recently occurred in Southern California in 1992, in Turkey in 1999, and in Taiwan in 1999 are presented to update the summaries found in papers published before these events.

3.2 Observations from the 1992 Landers, California Earthquake

The rupture zone produced by the 1992 Landers, California Earthquake (M_w = 7.3) is not a simple, linear fault trace as typically depicted in textbooks. Instead, a broad shear zone, often hundreds of meters wide with numerous individual fractures, represented the surface fault trace of the Landers event (Johnson et al. 1993, Lazarte et al. 1994). Although a majority of relative fault displacement occurred within a zone only 10 m wide or less, significant fractures and ground movements (on the order of a few centimeters – sufficient to be of engineering interest for many projects) were observed over a zone 100 m wide or more. At greater distances from the fault, minor ground movements (on the order of a few millimeters) were sometimes observed. These ground fractures, which were primarily extensional, are still a concern for some sensitive structures.

It is instructive to examine the characteristics of ground displacements across zones perpendicular to the strike of the main trace. An example of the mapping performed at several sites after the Landers event is shown in **Figure 3**. The ground ruptures at the Chaparral Site are primarily along and to the west of the main trace. Although a majority of relative movement is concentrated within a zone 2 m wide enveloping the main trace, significant ground fracturing is observed over a zone approximately 30 m wide. In **Figure 4**, the cumulative concentrated right-lateral horizontal offset across the Chaparral Site and three other mapped areas is shown. The two areas shown at the top of **Figure 4** (Acoma and Chaparral sites) represent locations along the well-defined Johnson Valley fault, where movement is concentrated along the main trace. The two areas shown at the bottom of **Figure 4** (Kickapoo sections

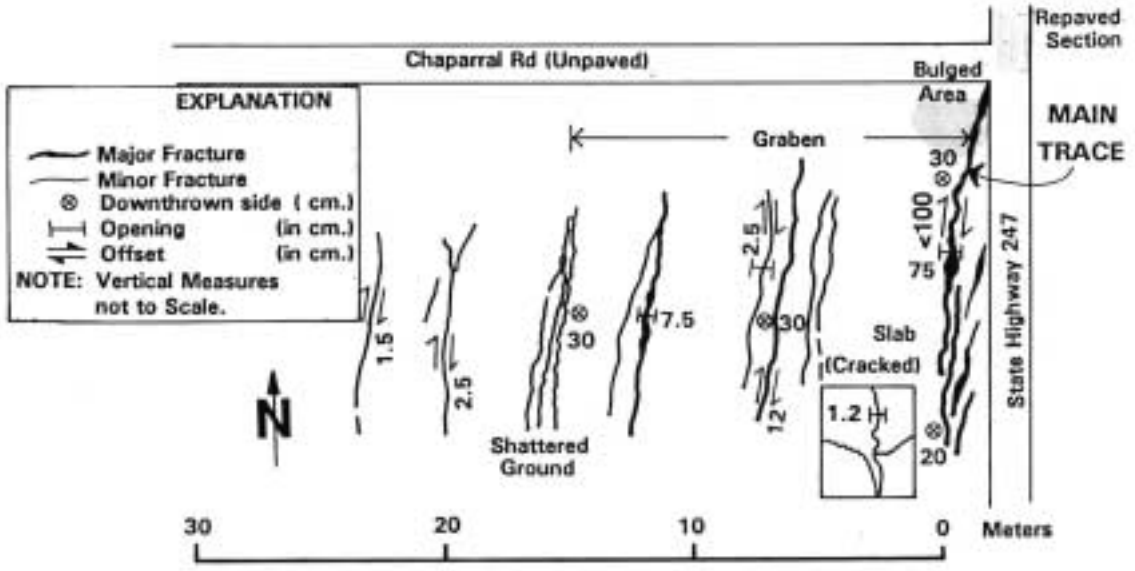

Figure 3 Distribution of ground rupture across the Johnson Valley fault at the Chaparral site (after Lazarte et al. 1994).

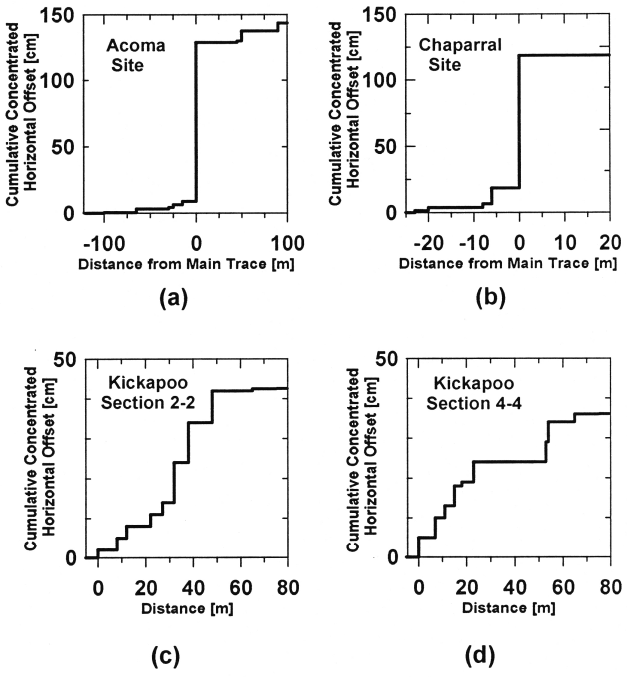

Figure 4 Cumulative concentrated right-lateral horizontal offset across selected zones:
(a) Acoma site,
(b) Chaparral site,
(c) Section 2-2 at the Kickapoo Trail Site, and
(d) Section 4-4 at the Kickapoo Trail Site (after Lazarte et al. 1994).

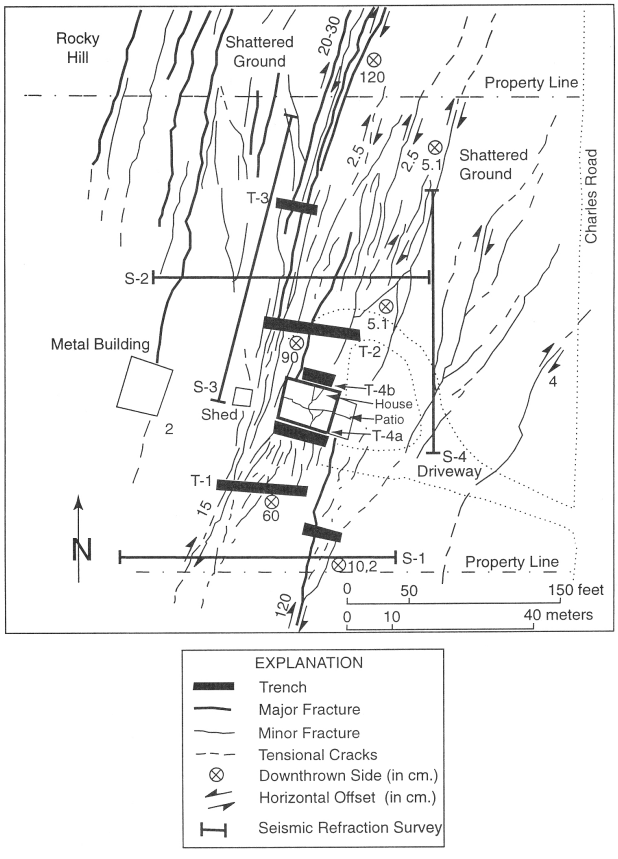

Figure 5 Ground ruptures and exploration locations at Lannom residence at northern end of the Kickapoo stepover (after Murbach et al. 1999).

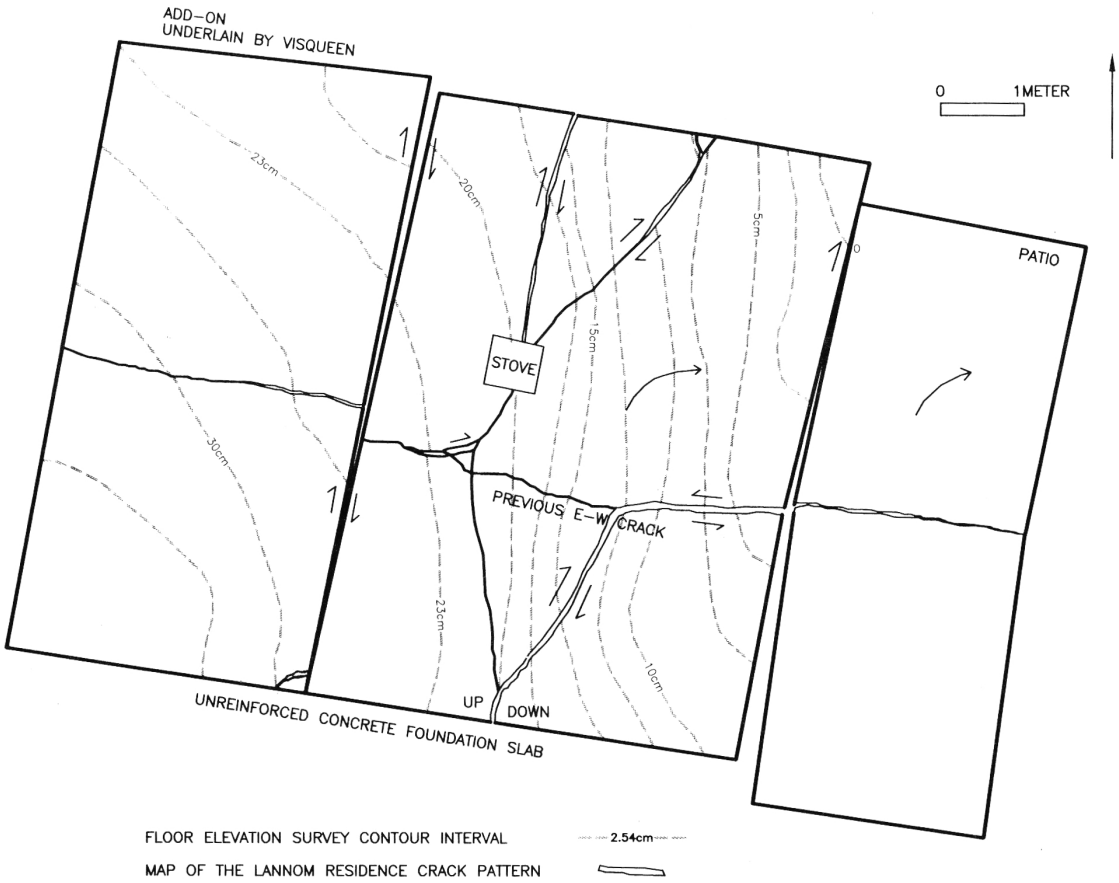

Figure 6 Deformation of foundation slab of Lannom residence. Left unreinforced concrete foundation slab is underlain with plastic (Visqueen) and right foundation slab is not underlain with plastic. Primary fault scarp is to the left of this building (after Murbach et al. 1999).

2-2 and 4-4) represent locations within the developing, less established Kickapoo stepover, where movement was distributed across a wide zone. These plots do not include the relative displacement between individual fractures resulting from ground distortion (i.e. simple shear deformation before development of distinct shear ruptures), and this ground distortion or warping may be important for some cases.

Stepover zones that develop between interacting fault segments are particularly important, because they are often difficult to identify a priori and are typically broader and more complex. For example, the Kickapoo Stepover Fault was not mapped as a zone containing active fault traces by the State of California as required by the Alquist-Priolo Earthquake Fault Studies Act until after the 1992 Landers event. Although attempting to identify active faults is worthwhile so that land use in areas that may undergo surface fault rupture can be limited or modified, the profession cannot rely solely on fault identification and setback, because our knowledge of faulting is imperfect and restricting land use excessively in urban areas is politically and economically untenable.

Several structures that were damaged by surface faulting were studied after the 1992 Landers Earthquake (Murbach et al. 1999). An example of a house impacted by surface faulting is shown in **Figure 5**. This is a remarkable case history, because fault trenches were excavated along the building foundation, which clearly showed how the underlying ground ruptures damaged the overlying building foundation. The building foundation condition was assessed through mapping and a floor elevation survey using a manometer (**Fig. 6**). Even though the western part of the house was closer to the main fault trace and overlaid larger ground fractures, it received less damaged. It appears that damage was limited due to a plastic sheet (Visqueen) underneath it that decoupled the foundation slab from the intense ground shearing underlying it. The plastic sheet limited the transfer of horizontal strain in the ground below the foundation to the slab, keeping the foundation slab in tact. Conversely, the other slab, which was not underlain by a plastic

sheet, was broken into several discrete blocks due to the nearly complete transfer of horizontal strain through the sandy soils below the foundation. Some horizontal shears were observed in the sand below the foundation, indicating that the soil began to fail as the ground deformation increased and the full strength of the sand stratum was mobilized. The weaker interface strength of the plastic allowed decoupling at an earlier stage of deformation than that in the sand stratum without the plastic sheet. The plastic decoupling layer "shielded" the overlying structure from some of the underlying ground strain.

Key findings from observations of surface fault rupture and its effects on structures from the 1992 Landers, California earthquake are particularly insightful (Lazarte et al. 1994, Murbach et al. 1999):

- Faults that were mapped on the surface from the 1992 surface rupture were difficult to recognize a year and a half later in the trenches excavated in coarse, cohesionless materials. Trench curing techniques played a key role in defining fault locations in trench exposures. These observations suggest that it may be difficult in some cases to assess fault activity with fault trenches prior to site development.

- The age and material properties of the alluvium influenced the pattern of deformation. Younger, less dense, more granular materials exhibited more vertical fractures and less distinct "flower structures". Denser, older alluvium displayed the most "flowering."

- The upward splaying pattern of the fault in the subsurface, as exposed in all trenches, suggests that the pattern of deformation in unconsolidated alluvium tends to spread out across a wider zone at the surface. The areas of thinner alluvium/shallower bedrock correlate to the areas of more narrowly constrained vertical surface displacement.

- Unreinforced concrete slabs underwent brittle failures as a result of direct fault displacement. Concrete slab cracks opened first in tension and then slipped laterally. Preexisting cracks and cold joints localized slip in the concrete foundation slabs. Where a vertical component was present, deformation was expressed primarily by tilting of the broken concrete slab pieces.

Figure 7 Apartment house shown on right side of photo, which collapsed due to surface rupture. Fault passes across the middle of the photo between the two standing apartment houses; the far apartment house has been offset about 3 m from its original alignment with the near apartment house (Photo by F. A. Swan from Lettis et al. 2000).

- The primary surface rupture features produced the most significant cracking in the foundation. However, many, less significant subsurface ground cracks did not fracture overlying concrete slabs (and most were unreinforced).

- Dextral movements produced clockwise rotation of the concrete slabs, and clockwise rotation and twisting of a steel electrical power transmission tower.

- Decoupling was observed below the concrete foundation that was underlain by plastic sheets, and partially through the subsurface sands below the concrete foundation without plastic sheets.

3.3 Observations from the 1999 Kocaeli and Duzce Turkey Earthquakes

Extensive surface rupture accompanied the August 17, 1999 Kocaeli, Turkey (M_w = 7.4) earthquake. Surface rupture consisted primarily of right-lateral strike-slip displacement averaging 3 to 4 m, with localized vertical displacements of up to 2.4 m (Lettis et al. 2000). The fault rupture produced classic examples of strike-slip offset, including well-formed mole tracks, left-stepping en-echelon fault traces at a variety of scales, uplift of pressure ridges, and subsidence of extensional pull-apart basins. The fault rupture traversed urban areas, producing excellent examples of the effects of

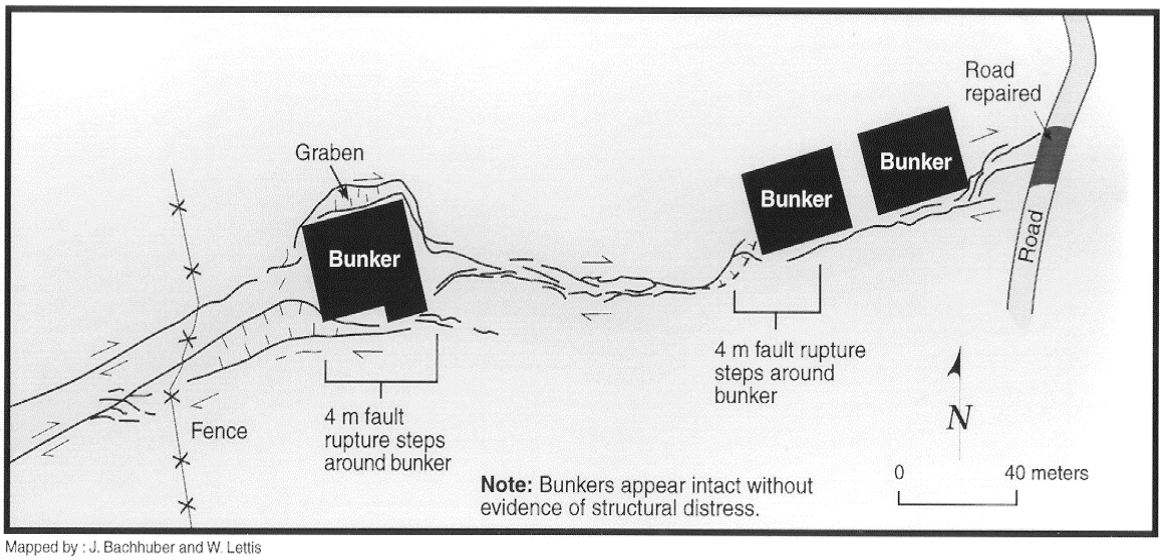

Figure 8 The stiff concrete bunkers shown in this map were not damaged by the surface fault rupture that was diverted around them (Mapped by J. Bachuber and W. Lettis; from Lettis et al. 2000).

surface fault rupture on engineered structures. The November 12, 1999 Duzce earthquake (M_w = 7.1) extended the surface rupture of the August event further to the east producing up to 4 m of right-lateral displacement with localized vertical movements. It too cut across towns and bridges, producing numerous examples of the effects of surface fault rupture on facilities. Detailed descriptions of these events are provided in earthquake reconnaissance reports such as Barka et al. (1999), Fumal et al. (1999), and Lettis et al. (2000). In this section, some particularly insightful records of building response to fault rupture from Lettis et al. (2000) and from the author's field notes are discussed.

Surface fault rupture often caused complete collapse or significant damage to buildings directly astride the fault trace. In particular, significant damage occurred along the Gölcük fault segment, where 4 to 5 m of surface rupture occurred. In the City of Gölcük, several reinforced concrete frame apartment buildings collapsed or were heavily damaged by fault rupture (**Fig. 7**). Surface fault rupture also damaged numerous buildings on the Gölcük Naval Base, with the collapse of a housing facilities resulting in a significant loss of life. However, a series of three buried bunkers at the base were not damaged. Fault rupture of 3 to 4 m directly intersected the bunkers, which appear to be constructed of heavily reinforced concrete. The massive concrete bunkers caused the surface rupture to go around the bunkers (**Fig. 8**). Farther to the east, fault rupture extended offshore and crossed a series of docks and port facilities. Displacement typically was transferred through the rigid structural

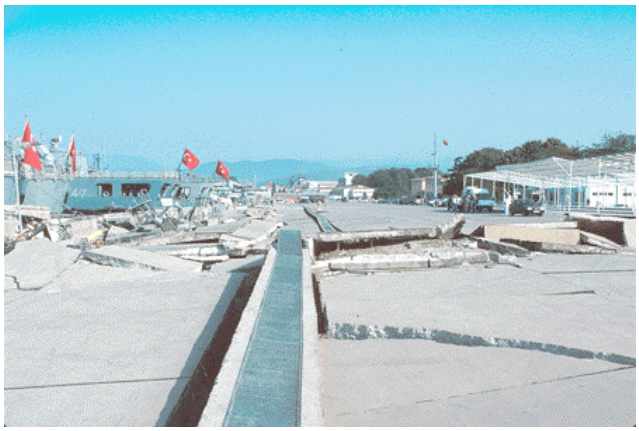

Figure 9 Fault offset of about 2 m heavily damaged this dock at the Gölcük Naval Base, which was fixed to the ground with piling (Photo by F.A. Swan; from Lettis et al. 2000).

members to weaker connections, joints, or elements of the docks, or was accommodated by global rotation, thereby spreading the damage over a wider area (**Fig. 9**).

The Gölcük pull-apart basin is formed due to the right-releasing stepover between the Gölcük and Sapanca fault segments. Surface fault rupture in this area was expressed by up to 2.4 m of vertical displacement along a normal fault through the city with widespread tectonic subsidence of the basin, which caused inundation along the coast. Several structures overlying the dip-slip fault displacement were heavily damaged due to extreme differential vertical ground movements (**Fig. 10a**). Approximately

(a)

(b)

Figure 10 (a) Extreme differential ground movement as a result of normal faulting in Golcuk destroys this apartment building; whereas, (b) apartment building that is located just off of fault scarp was not damaged, (Photos by J. D. Bray).

2.4 m of vertical displacement occurred within 1 m of a two-story concrete frame apartment building that was undamaged by fault rupture or by strong ground shaking (**Fig. 10b**). There were other cases of buildings in Gölcük located adjacent to the main trace which were only lightly damaged. However, buildings crossing the main trace often collapsed and some buildings located in subsidiary fault zones were heavily damaged by fault movement, such as a large assembly facility at the Ford-Otosan Plant.

Approximately 3 m of right-lateral displacement occurred on the Sapanca fault segment. In the City of Kullar, surface rupture occurred on two primary fault traces. On one fault trace, 2 m of lateral and

Figure 11 Fault rupture destroyed a primary school building in Kullar (Photo by L.S. Cluff; from Lettis et al. 2000).

Figure 12 Fault traversing beneath the corner of the Koran School, yet the school underwent only minimal damage (Photo by E. Rathje).

0.5 m of vertical displacement caused partial collapse of the town's primary school (**Fig. 11**). Strong ground shaking did not significantly damage surrounding buildings; thus, collapse of the primary school was most likely due to fault rupture. On the adjoining fault trace, about 1 m of lateral displacement directly intersected a two-story building. Displacement on the fault stopped at the building and slip was transferred to an adjoining, sub-parallel fault trace. About 1 km west of Lake Sapanca, the fault rupture directly intersects a school building (**Fig. 12**). About 1 to 2 m of distributed fault rupture was arrested by the building and forms a left en-echelon step around the building. The building foundation and walls were not damaged by the fault rupture.

Figure 13 Well-built 2-story house in Arifiye is not damaged although the primary surface fault scarp passed beneath it with over 3 m of right-lateral displacement. In response to the underlying fault movement, the stairs leading to the house have been offset relative to the house (Photo by J.D. Bray).

Approximately 3 to 5 m of right-lateral displacement occurred on the Sakarya fault segment. Fault rupture extended through several small towns. Within the Town of Arifiye, about 3 m of fault rupture extended beneath a 2-story residential house without damaging it (**Fig. 13**). The house foundation consisted of a shallow, 1 x 1 m reinforced concrete grid. Apparently, the shallow foundation was sufficiently stiff and strong to hold the building intact and to allow the foundation to decouple from the underlying alluvial soil on the south side of the fault. The decoupled side at the building was dragged about 2 m eastward by the north side of the fault. About 1 m of lateral displacement was consumed by compression of the soil along the margins of the house.

Fault rupture from the 1999 Duzce earthquake passed directly underneath the Bolu Viaduct, which is a state-of-the-art base-isolated bridge structure that was nearly complete at the time of the earthquake. Several meters of right-lateral fault displacement passed at an oblique angle through the viaduct. As shown in **Figure 14**, the ground movements rotated the pier relative to the deck it supports. The twisting of the pier foundation produced heaving of soil due to a passive earth pressure failure and ground cracking due to an active earth pressure failure on opposite corners of the foundation. The surface rupture, which followed a nearly linear path through this area, was diverted around the relatively strong embedded pier foundation. The fault rupture produced extensive damage to the viaduct, as the deck was displaced

(a)

(b)

Figure 14 Interaction of 1999 Duzce earthquake surface fault and Bolu Viaduct: (a) several meters of right-lateral fault rupture passes at oblique angle through viaduct and directly through one pier, (b) pier is twisted as shown but is not fractured as it rotates in response to underlying fault movement. Ground rupturing is diverted around pier (Photos by J. Bray).

relative to its support. The fault movement caused the base-isolators to undergo permanent displacement, and several deck sections nearly fell from their supports.

3.4 Observations from the 1999 Chi-Chi, Taiwan Earthquake

The 1999 Chi-Chi earthquake (M_w = 7.6) occurred along the Chelungpu reverse fault in central Taiwan, resulting in about 90 km of surface rupture (e.g. Chen et al. 1999, Chiu et al. 1999, Lee et al. 1999, and Ma et al. 1999). Severe damage occurred along

Figure 15 View to the east of surface fault rupture through Shihkang Dam (Photo by J.D. Bray).

Figure 16 Collapse of Highway 13 bridge north of Fengyuan due to 6 m fault movement (Photo by J.D. Bray).

the fault rupture, perhaps to a greater degree than in previous recent earthquakes along faults of all types throughout the world (Kelson et al. in press). The abundant building damage along the fault trace and secondary ruptures demonstrates that the location, width, and style of fault-related ground rupture strongly influenced the severity of earthquake damage. Several examples described in Kelson et al. (in press) with some additional personal field observations are presented below.

The fault rupture through the Shihkang Dam is a remarkable case (**Fig. 15**), because it represents the first time that a significant dam has been directly offset by primary fault rupture. A number of dams have been knowingly or unknowingly constructed atop potentially active fault traces, so this is an important case to study (Bray et al. 1992). Shihkang Dam was offset approximately 9 m near its right abutment due to primarily dip-slip rupture. In addition, the dam crest south of the failure experienced warping associated with a broad, west-trending anticlinal axis (Lee et al. 2000). This dam did not fail catastrophically, but it did lose its function of providing water supply for the City of Taichung.

Figure 17 Collapse of bridge directly east of Shihkang Dam due to tectonic compression (Photo by J.D. Bray).

Most bridges that were damaged during the Chi-Chi earthquake were damaged as a result of surface fault rupture. This possible seismic demand has often been neglected in bridge design. Three examples of damage are provided here. Northeast of Fengyuan, a 6-m-high fault scarp passed through the southern part of the Highway 13 bridge, resulting in differential uplift of the bridge foundations and collapse of the southern three spans (**Fig. 16**). The Wu Hsi Bridge (located about 7 km south of WuFeng along Highway 3) was traversed by up to 2 m of faulting. The bridge is actually composed of slightly different northbound and southbound bridges. The northbound bridge had spans that were pushed off their supports by robust concrete piers that moved as the ground moved. Conversely, the weaker piers of the southbound bridge failed in shear, so that only part of the underlying ground movement was transferred to the spans, which did not collapse. Additionally, the characteristics of the surface rupture were affected by the stiff concrete piers that caused the surface rupture to splay around them, forming two distinct scarps rather than the single, well-defined scarp away from the bridge. Finally, east of Shihkang Dam, an eleven-span bridge collapsed due to tectonic compression across the bridge from what appears

Figure 18 Fault scarp that is about 5 m high passes close to, but does not damage, a simple steel-framed warehouse that is located on footwall side of shallow thrust fault (Photo by J. Bray).

Figure 19 The primary trace of the Chelungpu fault passed beneath this apartment building in Wu Feng, producing about 2 m of vertical displacement through the building (Photo by K. Kelson).

to be two poorly expressed opposite dipping reverse faults near each bridge abutment (**Fig. 17**).

With regard to building damage, there was relatively little differential ground deformation on the footwall block and consequently less building damage (**Fig. 18**). Those buildings that were damaged were pushed laterally when the hanging-wall thrust over the footwall, but this occurred only in close proximity of the main fault trace. Buildings straddling the fault trace underwent severe differential ground movements and were typically heavily damaged (**Fig. 19**). However, significant ground deformation expressed by warping or secondary ruptures occurred on the hanging-wall, and this damaged many buildings situated on the

Figure 20 North-facing subsidiary fault in hanging-wall block and local ground deformation damages this house and warehouse. This site is located southeast of Shihkang Dam and south of the primary fault ruptures running along the Tachia River in this area (Photo by J. Bray).

hanging-wall (**Fig. 20**). Ground deformation was greatest along the fault scarp and about 20 m from it on the hanging wall, but significant ground deformation was observed as much as 100 m from the fault scrap and further when back-thrust faults displaced hundreds of meters from the fault scarp on the hanging-wall block. Where the surface deformation was dominated by anticlinal folding, building damage occurred over a substantially broader area. The wider zone of severe building damage appears to be a result of the broader width of ground deformation in the hanging-wall anticline. These observations along with similar observations from other reverse fault events (e.g. Bray et al. 1994a) indicate that building zonation along reverse faults should be asymmetric, with narrow setbacks being appropriate on the footwall side and wide setbacks being necessary on the hanging-wall side.

4. ANALYTICAL PROCEDURES FOR INVESTIGATING SURFACE FAULT RUPTURE

4.1 Finite element method

Previous numerical studies of fault rupture propagation through earth materials suggest that the finite element method can be applied to this class of problems provided an incremental nonlinear stress-strain soil behavior model is employed (e.g. Bray et al. 1994b, Lazarte 1996). Finite element programs, such as GeoFEAP (Espinoza et al. 1995) and

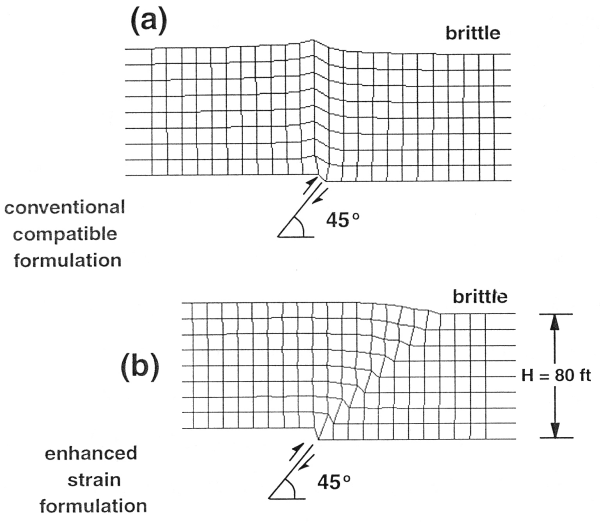

Figure 21 Improved performance of enhanced strain element compared to conventional compatible formulated element for modeling response of saturated clay to 45 degree reverse fault displacement (after Lazarte 1996).

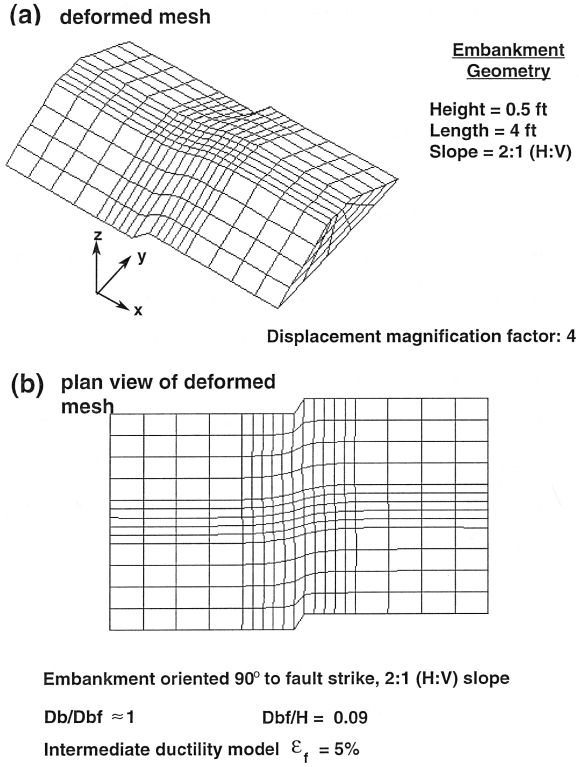

Figure 22 Three-dimensional finite element analysis of physical model experiment investigating the response of saturated clay embankment to foundation strike-slip fault movement (after Lazarte 1996).

SSCOMPPC (Boulanger et al. 1991), have been employed. These programs are general soil-structure interaction finite element analysis computer programs modified for geotechnical applications (Zienkiewicz & Taylor 1989).

The use of nonlinear soil constitutive models is required in this application (Bray et al. 1994b). The Duncan et al. (1980) model is one of the most widely used nonlinear stress-dependent soil constitutive models, and has been used in numerous finite element analyses of earth structures ranging from earth dams to soil reinforced walls. The hyperbolic model characteristics and limitations are described in detail in Duncan et al. (1980). Its use in solving boundary deformation problems such as earthquake fault rupture propagation is described in Bray et al. (1994b). The Duncan hyperbolic model can represent the nonlinear stress-dependent stress-strain and volumetric response of soils using the Mohr-Coulomb failure criterion, an instantaneous tangent Young's modulus that increases with confining stress but decreases with stress level as soil approaches failure, and an instantaneous bulk modulus that increases with confining stress. In all, 8 soil parameters are used which can be developed with standard procedures from triaxial test data. The major advantage of this model in this application is that the analyst can control the failure strain of the soil. Failure strain, as opposed to strength, is the most important soil response characteristic to capture in the earthquake fault rupture problem. Numerous studies have shown that this model can capture the response observed in physical model tests, and it offers significant advantages compared to other models due to its ability to capture controlled variations of the soil's failure strain.

Recent developments in finite element technology, however, enable the analyst to employ more robust methods, such as the enhanced strain element developed by Simo et al. (1993). As shown in **Figure 21**, an enhanced strain formulation can eliminate the problem of mesh locking that sometimes results when using a conventional compatible finite element formulation with a material that is undergoing constant volume shear deformation. Analysis of an embankment composed of saturated clay using the enhanced strain formulation allowed for better representation of the localized deformation that occurs once the base displacement has propagated a shear rupture up to the ground surface (Lazarte 1996). For example, the general trends expressed in the physical model experiments described in Lazarte & Bray (1996) were essentially captured by the finite element analyses performed by Lazarte (1996) as shown in **Figure 22**.

4.2 Discrete particle method

Performance-based engineering, where the focus is on deformation, not strength, begs for a revolutionary approach in the assessment of the seismic response of earth structures, such as dams, to earthquake fault rupture. It has long been known that the particulate nature of soil influences its mechanical response (e.g. Mitchell 1976). However, the response of earth structures has been traditionally modeled using continuum mechanic techniques, such as the finite element method. Recent advances in computational equipment and procedures have made discrete modeling of granular materials possible using Distinct Element Methods pioneered by Cundall & Strack (1979) and using Discontinuous Deformation Analysis pioneered by Shi & Goodman (1989) and first applied to soil by Ke & Bray (1995). Discrete particle techniques have been shown to model the micro-mechanics of particle assemblies well, and these techniques offer a revolutionary way to investigate the particulate response of soil. These approaches are especially useful when examining the particulate nature of soil undergoing failure (Thomas & Bray 1999). Unfortunately, major advances in this area are hindered by the computational effort still required to solve problems involving just a few thousand two-dimensional disk-type particles, so widespread use of discrete particle methods will not occur until orders of magnitude of improvement in computational speed is achieved and the method undergoes critical validation.

5. MITIGATION MEASURES FOR SURFACE FAULT RUPTURE

There are three principal means of mitigating the potential hazards associated with earthquake fault rupture: avoidance, geotechnical engineering, and structural engineering. The success of each of these approaches depends, first and foremost, on proper interpretation of the geology on regional and project level scales. Although the profession requires continual enhancement of its understanding of the complex fault rupture phenomenon, sound judgment, coupled with reasonable interpretations of surficial geology and crack propagation theory, can be applied to develop earthquake-resistant designs without resorting to arbitrary, specified setback criteria. More realistic criteria can be established on a project/site-specific basis (e.g. Bray et al. 1993a). Once detailed studies of the geology and local site conditions (soil and topography) are completed, a combination of the methods described below may be employed to reduce damage resulting from surface rupturing.

The first approach is avoidance. All structures and lifelines may be deliberately positioned to avoid crossing identified shear rupture zones. Obviously, this method's success depends on identifying all likely rupture zones, and on the characteristics of the next earthquake complying with our expectations. Recent earthquakes provide numerous examples of our imperfect understanding, and show that some movement should be anticipated throughout fault zones. For example, Hart et al. (1993) noted that 45% of all 1992 Landers earthquake surface ruptures fell outside established A-P Earthquake Fault Zones that delineate "approximately wide . . . zones to encompass all potentially and recently active [fault] traces." In another study of over 1200 active faults strands exposed in fault trenches, Bonilla & Lienkaemper (1991) found that about 45% of these strands either appeared to die out, or actually did die out, even though surface faulting was known to have occurred recently. They concluded that a fault strand overlain by an apparently undisturbed deposit is not necessarily older than the deposit.

The next approach is to use the inherent capability of unconsolidated geomaterials to "locally absorb" and distribute distinct bedrock fault movements. Previous field, physical model, and numerical studies (e.g. Bray et al. 1994a,b) have found that differential movement across distinct bedrock faults dissipates as the shear rupture plane rises through overlying fills, especially if the fills are reinforced (Bray et al. 1993a). The relative displacement across a distinct bedrock fault is spread across a wider zone in the overlying fill. This spreading of the localized bedrock fault displacement over a wider zone at the ground surface reduces differential settlement and tensile strain at this level. Hence, ductile compacted fill or reinforced fill may be used at a site to mitigate the surficial hazards associated with fault rupture.

Finally, the constructed facility can be engineered to undergo some limited amount of ground deformation without collapse or significant structural damage. Design of structures subjected to ground deformation resulting from mining subsidence are applicable (e.g. Kratzsch 1983). Similar to observations of foundation performance undergoing fault rupture, mining subsidence studies indicate that foundation elements should be reinforced to improve ductility. The maximum allowable tilt for conventional structures is approximately 1/400, but specially built structures can tolerate more. The maximum allowable horizontal tensile ground strain below buildings is on the order of 0.3%. Post-tensioning the floor slab will improve its ability to bridge over irregular

ground deformation of limited extent. Spread footings and floor slabs should be constructed atop a double layer of smoothly laid-out polyethylene (plastic) sheets sandwiched between layers of clean coarse sand to fine gravel. This measure will reduce the extent of tensile cracks just below the building's foundation and minimize the transfer of horizontal strains in the ground below the foundation to the structural foundation elements. Trenches excavated to construct grade beams and underground utilities should be backfilled with loose soil or styrofoam to reduce lateral earth pressures developed against these elements.

6. EVALUATING AND IMPLEMENTING FAULT RUPTURE MITIGATION DESIGN MEASURES: AN ILLUSTRATIVE PROJECT

6.1 Introduction

The project site to be discussed is located in Ventura County, Southern California. The site is situated between a tectonically uplifted mountain range due to folding and reverse slip on the south-dipping Oak Ridge fault to the north of the site and the north-dipping Simi-Santa Rosa fault system that has produced uplift of hills to the south of the site. Quaternary deposits at the site have been displaced due to folding and faulting. However, clear evidence of distinct surface faulting through Holocene materials at the site could not be established. Hence, fault features were not necessarily active (i.e. surface fault displacement within the last 11,000 years). Moreover, the project site is not located within an A-P Earthquake Fault Study Zone, where special restrictions apply through the State of California Alquist-Priolo Act. However, the project developer and regulator agreed that it would be prudent to utilize geologic and engineering studies to address the hazards associated with surface fault rupture, because the geology was sufficiently complex and poorly defined to rule out the possibility of surface faulting.

Geologic field studies performed at the project site indicate that the characteristics of bedrock faults vary across the project site, but the faults can be grouped into two general categories: (1) shallow thrust faults that dip from about 10 to 30 degrees, and (2) hanging-wall bending moment normal faults with representative dips of 65 and 85 degrees. Several cross sections, with representative soil thickness varying from 3 m to 30 m, that capture the primary characteristics of the faults at the project site were developed working with the project geologist, along with ranges of possible bedrock fault displacements for each fault.

6.2 Project performance criteria

It is assumed that functionality, not "no damage," is the project objective for seismic performance of engineered systems. This project objective is actually more stringent than how the Uniform Building Code in America addresses the earthquake shaking hazard (e.g. effective ground accelerations are median values, not maximum values, at the 10% probability of exceedance in 50 year level and the purpose of the code is to safeguard against major structural failures and loss of life, not to limit damage or maintain function). It would be difficult and inconsistent with standard practice to design houses to withstand design earthquake events (both minor bedrock fault movements and strong ground shaking) without incurring some damage, such as cracking in drywall, plaster, and brickwork. Consideration should be given to developing a design philosophy for the surface fault rupture hazard that is consistent with that developed for the ground shaking hazard and for other seismic hazards. However, at this time, government regulators typically require more stringent performance criteria for the surface fault rupture hazard.

Consequently, it was decided that setbacks would be necessary in areas where the fault rupture might reach the ground surface. Most of the rupturing of buried faults may be contained within the overlying soil and hence, only cause warping of the ground surface. At some locations, over-excavation may be required to construct compacted fill over the bedrock faults to mitigate the surficial hazards associated with base rock fault displacements. The depth of over-excavation should be minimized, however, to reduce the potentially deleterious effects of the other more routine design considerations (e.g. shrink/swell/collapse under static service loads, and vibration induced settlement under earthquake ground shaking). The results of previous investigations (e.g. Bray 1990, Lazarte 1996) suggest that dip-slip fault movements (especially normal faults which induce extensional strains within the overlying soil) pose a greater hazard than strike-slip fault movements. Hence, two-dimensional (2D), plane strain, finite element analyses (FEA) of dip-slip base rock fault displacements (both reverse and normal) are investigated.

Regarding the principal hazards of bedrock fault displacements described previously, the potentially most damaging of these hazards is Hazard A (propagation of the distinct shear rupture plane to the ground surface), and areas where this hazard is likely should be engineered to withstand this surface offset satisfactorily. In general, housing should not

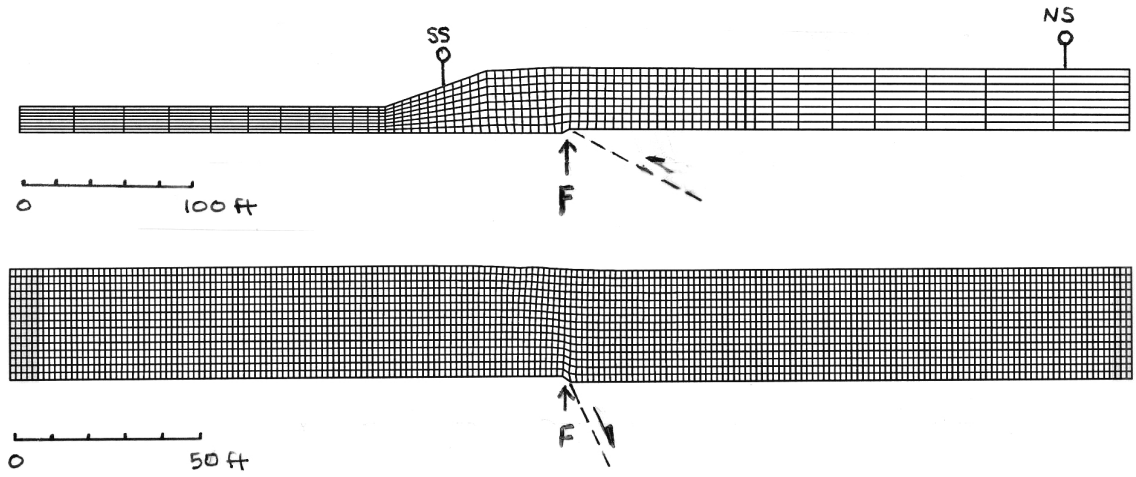

Figure 23 Finite element meshes representing soil overlying shallow thrust fault rupture (Section R-R' shown at top) and hanging-wall bending moment normal fault rupture (Section X-X' for 65^o dipping normal fault shown at bottom). Meshes drawn with scale of 10 ft = 3.05 m. "F" denotes tip of bedrock fault, and "SS" and "NS" denote south and north setbacks, respectively.

be constructed over ground that could undergo surface fault rupture, although lifelines (e.g. roads and utilities) will necessarily have to traverse ground that could undergo surface fault rupture. This is consistent with the manner in which more significant faults (i.e. higher slip rate and larger ground rupture potential) are handled in the State of California, in which the siting of new facilities for human occupancy over active faults designated by the California Division of Mines and Geology is avoided, but it is unavoidable that some lifelines might have to cross active faults. The appropriateness of the setbacks preliminarily developed by the project geologist could be assessed though analysis of reasonable fault rupture scenarios.

As most of the base rock displacements at this project site are "absorbed" within the overlying in situ alluvium and compacted fills, Hazards B and C will largely determine if the proposed setbacks are satisfactory. Moreover, in areas outside of the "Restricted Use Zones (RUZ)" designated by the proposed setbacks, Hazards B and C will govern the recommendations of minimum structural fill thickness to mitigate the earthquake fault rupture scenario, as surface fault rupture (Hazard A) is judged to be not acceptable for areas where houses may be sited. For Hazard B, the maximum angular distortion over a reasonable length (6 m) is initially taken as 1/360. Since post-tensioned foundation slabs were being recommended, this conforms to standard practice in southern California. For Hazard C, based on accepted mining subsidence practices and appropriate foundation design provisions (e.g. Kratzsch 1983, Chen 1988, Whittaker & Reddish 1989), the maximum horizontal tensile strain in the soil is initially taken as 0.3 percent.

These numbers are for conventional structures, but may be modified based on the incorporation of structural engineering mitigation measures. The tolerable criteria is intimately linked to the ductility of the structure and the manner that the foundation is coupled to the ground. As discussed previously, effective ground deformation often includes mitigation through geotechnical engineering measures, such as increasing the fill height and fill ductility, and through structural engineering measures, such as thickening and improving structural detailing of reinforced concrete foundations.

6.3 Analysis

The plane strain FE computer programs GeoFEAP (Espinoza et al. 1995) and SSCOMPPC (Boulanger et al. 1991), which employ an incremental load solution technique with the Duncan et al. (1980) hyperbolic soil behavior model, were utilized in this study to model the nonlinear stress-dependent response of reinforced compacted soils. The principal advantages of these programs are that they allow discrete modeling of the soil, the reinforcement, and the soil-reinforcement interface, and these programs are well validated. Representative finite element models of the two primary fault scenarios anticipated (i.e. shallow thrust faulting and steeply dipping normal faulting on the hanging-wall of these thrust faults) are shown in **Figure 23**. The fault tip (denoted by the letter "F" in the figures) is used as the reference point for

Table 1 Hyperbolic Soil Model Parameters For Fill Materials and In Situ Alluvium.

Soil Case	Soil Type and State	ε_f (%)	c (kPa)	ϕ (deg)	$\Delta\phi$ (deg)	K	n	R_f	γ (kN/m^3)
A	S1, MC=Opt+3%, RC=92%	5 - 9	21	40	0	1200	1.25	0.98	20
B	S1, MC=Opt+1%, RC=97%	2 - 3	24	45	5.7	1800	0.59	0.925	20
C	S2, MC=Opt+6%, RC=90%	11 - 13	16	29.5	0	410	0.62	1.0	20
D	S2, MC=Opt+2%, RC=96%	6 - 6.5	24	38.5	12.6	1000	0.47	0.98	20
E	S3, MC=5%, γ_d = 115 - 120 pcf	6 - 7	23	34	0	900	0.53	0.99	21
F	estimated S1, RC=95%	3.5 - 4	24	42	0	1500	0.8	0.96	20

Notes: (1) ε_f = failure strain determined from triaxial compression test
(2) K_{ur} = 1.5 * K; K_b = 1.5 * K and m = n so that ν_i = 0.4
(3) RC = relative compaction using ASTM D1557 as standard
(4) MC = moisture content relative to ASTM D 1557 optimum
(5) S1 = Older Alluvial Fill, S2 = Holocene Alluvial Fill, and S3 = In Situ Older Alluvium

locating zones of high tensile strains and angular distortions. Distances are provided as north or south of the vertical projection of the tip of the fault.

A program of laboratory testing was developed to evaluate the stress-strain responses of the predominant materials at the project site. A series of anisotropically consolidated undrained triaxial compression tests were performed with partially saturated soil specimens. Triaxial tests were performed on samples believed to be representative of the in situ alluvium, and triaxial tests were performed on reconstituted specimens believed to be representative of the fill materials to be used at the project site. The USCS soil classifications of the materials are: SW-SM for the in situ alluvium, SW-SM for the older alluvium used as fill, and SM for the Holocene alluvium used as fill. The in situ alluvium and older alluvial fill were identified as being the predominant materials on site. The strain rate during undrained shear was set deliberately high (around 20%/hr) to simulate at least qualitatively the high strain rates imposed by an earthquake base rock fault displacement.

Although shear strength is often a key issue, in boundary deformation problems, the controlling issue is material ductility as expressed as the axial strain at failure or failure strain (i.e. axial strain at maximum deviator stress; see Bray et al. 1994b). The measured failure strain of these materials ranged from 6% to 7% for the in situ alluvium, from 2% to 9% for the older alluvial fill, and from 6% to 13% for the Holocene fill. Lower failure strain values were observed at the higher relative compaction levels (R.C. = 96-97%), and higher failure strain values were observed at the lower relative compaction levels (R.C. = 90-92%).

Duncan et al. (1980) hyperbolic soil model parameters were developed for each test series, and these parameters are presented in **Table 1**. Soil A represents the older alluvial fill at a relative compaction of 92%; Soil B represents the older alluvial at a relative compaction of 97%; Soil C represents the Holocene alluvial fill at a relative compaction of 90%; Soil D represents the Holocene alluvial fill at a relative compaction of 96%; and Soil E represents the in situ older alluvium. In general, the model represented the in situ alluvium and compacted fill stress-strain responses well. These model parameters are consistent with those used on other projects (see Duncan et al. 1980), with the exception that these model parameters display relatively stiff stress-strain responses (i.e. high modulus numbers, K) due to the faster strain rates of these tests. To aid in the sensitivity analyses, soil model parameters for Soil F, which represents the older alluvial fill at a relative compaction of 95%, were developed based on a straightforward interpolation of the soil parameters for Soils A and B.

6.4 Results

(1) *Shallow thrust faults*

Representative results of the finite element analysis of some cross sections representing the shallow thrust faults are provided in **Table 2**. The cross section analyzed is given in the first column, and it refers to a designation given by the project geologist. The soil case (Soil Case A-F; see **Table 1**) used in the analysis is given in the second column with the height of soil above the fault tip provided in the third column of the table. The amount of base rock fault offset is given in the fourth column. The height that the shear zone rises above the base rock fault tip is given in the fifth column. Hazard B can be evaluated studying the sixth and seventh columns,

Table 2 Results of Finite Element Analysis for Some Shallow Thrust Faults (Unreinforced Soil).

Section	Soil	Soil/Fill Thickness (m)	Base Fault Offset (cm)	Hazard A Ht. of Shear zone (m)	Hazard B Max. Angular Distortion (over 6 m)	Hazard B Location of zone >1/480[(1)] (m)	Hazard C Max. Tensile Strain (%)
R-R'	E	11	15	1.5	1/165	18 s to 0.0	0.39
R-R'	E	11	7.5	< 0.5	1/380	11 s to 58 s	< 0.3
V-V'	B	17	15	< 0.5	1/365	21 s to 12 s	0.47
V-V'	B	17	7.5	< 0.5	1/1000	none	< 0.3
V-V'	D	17	15	< 0.5	1/450	20 s to 13 s	0.45
V-V'	D	17	7.5	< 0.5	1/1140	none	< 0.3
P-P'	A	5	10	1	1/120	10 s to 1 s	0.89
P-P'	A	5	5	< 0.5	1/260	7 s to 1 s	0.35
P-P'	B	5	10	5	1/110	10 s to 2 s	1.1
P-P'	B	5	5	1.5	1/240	8 s to 2 s	0.45
P-P'	C	5	10	0.5	1/120	9 s to 1 n	0.87
Q-Q'	B	18	10	0.8	1/580	none	< 0.3
Q-Q'	B	18	5	< 0.5	1/1600	none	< 0.3
Q-Q'	D	18	10	< 0.5	1/970	none	< 0.3

Note: (1) Distances given are relative to the vertical projection of the bedrock fault tip with "s" representing south (to left of mesh shown) and "n" representing north (to right).

which provide the maximum angular distortion at the ground surface over a horizontal distance of 6 m and location of the zone (relative to the vertical projection of the bedrock fault tip) of large angular distortion (i.e. > 1/480), respectively. The maximum tensile ground strain at the surface is given in the last column.

Reviewing **Table 2**, Hazard A (propagation of the distinct fault rupture to the ground surface) is found to be satisfactorily contained for most cases. The finite element results indicate that even in the "Restricted Use Zones" (RUZ) with these depths of soil at the specified base rock displacements, the distinct shear rupture is "absorbed" within the soil and surface rupturing is unlikely. One exception is for cross section P-P', where for the upper bound 10 cm base rock offset and the most brittle soil (Soil B), the shear rupture zone reaches the ground surface. This surface rupture zone is contained in the proposed RUZ, and the surface offset associated with this upper bound base rock displacement should be minor. The other exception, which is not presented in **Table 2**, is for the Southern Thrust fault, where a 28 cm thrust fault displacement produces surface ruptures at a base of a slope. Housing is not allowed in this area, and it is within a designated RUZ. If lifelines must traverse this zone, they would need to be engineered to accommodate a centimeter or so of surface offset. Reducing the slope from 3.3H:1V to 4.5H:1V, reduces the shear rupture hazard significantly (i.e. analyses now indicate the bedrock offset is "absorbed" in the fill), and makes the deformed slope more stable (i.e. equivalent FS > 1.5).

Significant angular distortions (i.e. > 1/360; Hazard B) are developed at the ground surface for a number of the faulting scenarios analyzed. However, the zones of significant angular distortions are contained within the proposed RUZ. In fact, the angular distortions calculated at the proposed setbacks are quite low (< 1/1000 and often < 1/10,000) for the faulting scenarios considered in this study. Hence, setback locations could be reduced significantly for most cases.

Significant tensile strains (i.e. > 0.3%; Hazard C) are developed near the ground surface for a number of the faulting scenarios analyzed. However, except for one case, the zones of significant tensile strains are contained within the proposed RUZ. Moreover, these zones are typically less than 10 m wide and developed only for the upper bound base rock fault displacements. The notable exception is for the slope offset by the Southern Thrust fault, where about a 25 m wide zone of high tensile strains (with

Table 3 Results of Finite Element Analysis of Unreinforced and Reinforced Fill for Some Hanging-Wall Bending Moment Faults.

Section	**Soil and Reinforcement Conditions**	**Soil/Fill Thickness** (m)	**Base Fault Offset** (cm)	**Hazard A** Ht. of Shear zone (m)	**Hazard B** Max. Angular Distortion (over 6 m)	**Hazard C** Max. (& Average) Tensile Strain (%)
X-X'	B	3	2.8 (65^0 NF)	3	1/240	1.4 (0.4 over 3 m)
X-X'	B	3	2.8 (85^0 NF)	3	1/220	0.7 (0.2 over 3 m)
X-X'	B - 2 Reinf.	3	2.8 (65^0 NF)	< 3	1/260	0.4 (0.15 over 3 m)
X-X'	B - 2 Reinf.	3	2.8 (85^0 NF)	< 3	1/220	0.4 (0.1 over 3 m)
X-X'	B	4.5	2.8 (65^0 NF)	4	1/260	0.8 (0.4 over 3 m)
X-X'	B	4.5	2.8 (85^0 NF)	4	1/230	0.4 (0.2 over 3 m)
X-X'	B - 2 Reinf.	4.5	2.8 (65^0 NF)	< 3	1/310	< 0.3
X-X'	B - 2 Reinf.	4.5	2.8 (85^0 NF)	< 3	1/260	< 0.3
X-X'	B	6	2.8 (65^0 NF)	5	1/280	0.45 (0.2 over 3 m)
X-X'	B	6	2.8 (85^0 NF)	5	1/260	< 0.3
X-X'	B - 2 Reinf.	6	2.8 (65^0 NF)	< 3	1/390	< 0.3
X-X'	B - 2 Reinf.	6	2.8 (85^0 NF)	< 3	1/330	< 0.3
X-X'	B - 2 Reinf.	7	2.8 (85^0 NF)	< 3	1/360	< 0.3
X-X’	A	9	2.8 (85^0 NF)	0.6	1/370	< 0.25
X-X’	B	9	2.8 (85^0 NF)	3	1/330	< 0.3
X-X’	C	9	2.8 (85^0 NF)	0.3	1/380	< 0.25
X-X’	D	9	2.8 (85^0 NF)	0.6	1/370	< 0.2
X-X’	E	9	2.8 (85^0 NF)	0.6	1/370	< 0.3
X-X’	F	9	2.8 (85^0 NF)	1.2	1/360	< 0.25

1.1% maximum) was calculated at the toe of the slope near the projection of the underlying thrust fault. Due to the fault rupture hazard discussed previously, as well as these high tensile strains, the slope was laid back from 3.3H:1V to 4.5H:1V. This reduced the tensile strain levels significantly. The maximum tensile strain now only slightly exceeded the 0.3% performance criteria for housing. Still, construction of housing in this zone of higher tensile strains should be avoided, but utilities and other lifelines should be able to be engineered to accommodate this level of straining satisfactorily.

(2) *Hanging-wall normal faults*

Results of the finite analysis of the case where bedrock hanging-wall bending moment normal faults are exposed during grading are summarized in **Table 3**. **Table 3** is organized similar to **Table 2**. Both normal faults that dip 65^o and 85^o are considered. Examples of the ground deformation patterns, stress level concentrations, and tensile strain distributions calculated by the finite element method for one of these cases are shown in **Figure 24**.

At the bottom of **Table 3**, the sensitivity of the results to varying the soil type and compaction conditions (Soil Cases A through F of **Table 1**) are presented for a given fill thickness and fault scenario. As shown at the bottom of **Table 3**, Soil Case B represents the worst case in terms of all hazards, especially Hazard A. This is consistent with the results from previous studies as shown previously in **Figure 2**. Brittle soil responses (i.e. lower failure strains, such as with Soil B) caused the shear rupture to propagate further at the same magnitude of base displacement. Hence, improving the ductility of the fill is desirable. This can be achieved by limiting the maximum density of the older alluvial fill, using the Holocene fill in critical areas, or by reinforcing the fill with geogrid-type reinforcement. In this paper, the remaining results in **Table 3** are only given for the worst soil case, i.e.

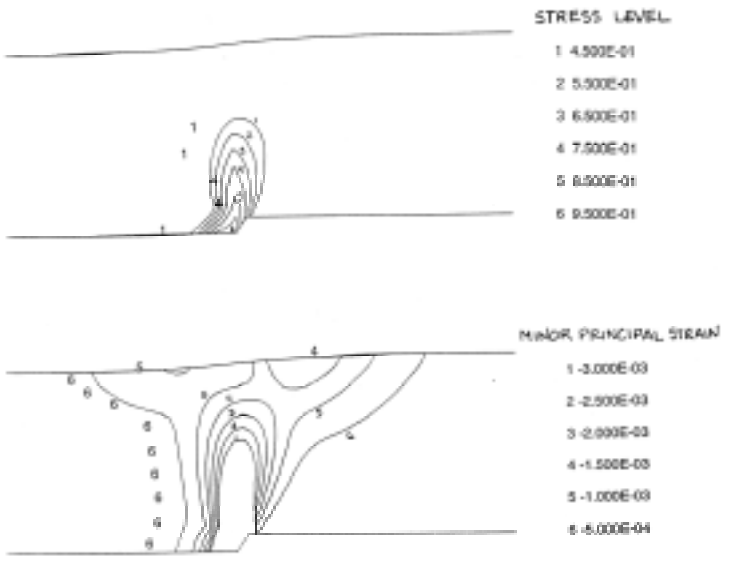

Figure 24 Partial results from finite element analysis of Section X-X', which is a 30 ft (9 m)-high unreinforced older alluvial fill material compacted at a relative compaction of 92% (Soil Case A), for the case of a normal fault offset of 2.8 cm.
Stress level = $(\sigma_1 - \sigma_3)/(\sigma_{1f} - \sigma_{3f})$.

Soil B, which represents the most brittle soil response with failure strains in the range of 2% to 3%, and the effectiveness of soil reinforcement is explored.

Reviewing **Table 3** further, propagation of the distinct fault rupture to the ground surface (Hazard A) is found to be an issue for Soil Case B when the fill is not reinforced and less than 9 m thick. The results indicate that as the fill height increases, the hazards associated with earthquake fault rupture are minimized. Significant angular distortions (i.e. > 1/360; Hazard B) are developed at the ground surface for cases where the unreinforced fill height is less than about 9 m. The near vertical 85° dipping normal fault is the most critical faulting scenario for satisfying the angular distortion performance criterion. The results are relatively insensitive to variations of the soil type. At fill heights of 6 m and 3 m, the maximum angular distortion values increase to approximately 1/300 and 1/200, respectively. Once again, fill height is found to be a controlling factor in reducing angular distortion at the ground surface for the base rock fault displacements specified in this study. Significant tensile strains (i.e. > 0.3%; Hazard C) are developed near the ground surface for cases where the fill height is 8 m or less. High tensile strains are localized in a fairly narrow zone of extension at the ground surface. The average minor principal strain calculated over a distance of 3 m is only about 0.2% for the 6 m-thick unreinforced fill cases shown in **Table 3**, which had maximum tensile strains of 0.45%. In addition, it is likely that (and in fact the foundation can be modified so that) the full horizontal strain developed in the soil below the foundation will not be transferred to the structural foundation.

The finite element mesh was modified to include up to eight layers of reinforcement. Tensar Geogrid material properties (UX1400HS-type with EA of approximately 450 kN and Long Term Allowable Design Strength of approximately 30 kN/m) were modeled as linear elastic bar elements that sustained only significant tensile forces. The soil-geogrid interface was modeled as a nonlinear stress-dependent zero thickness element that controlled the relative displacement of adjacent soil and structural element nodal points (Clough & Duncan 1969). The hyperbolic model parameters selected to model the soil-geogrid interface were based on a soil-geogrid interaction coefficient of 0.9 to 1.0. Similar to the results presented by Bray et al. (1993a), the finite element results were insensitive to reasonable variations in the geogrid tensile properties and soil-geogrid interface properties, but a minimum allowable design strength of 22 kN/m was necessary with at least two geogrid layers. If this criteria was met, rupture of the geogrid reinforcement was not likely, and the assumption of a linear elastic geogrid bar response was reasonable.

A series of finite element analyses were performed to investigate the effectiveness of soil-reinforcement for this project, and representative results for the

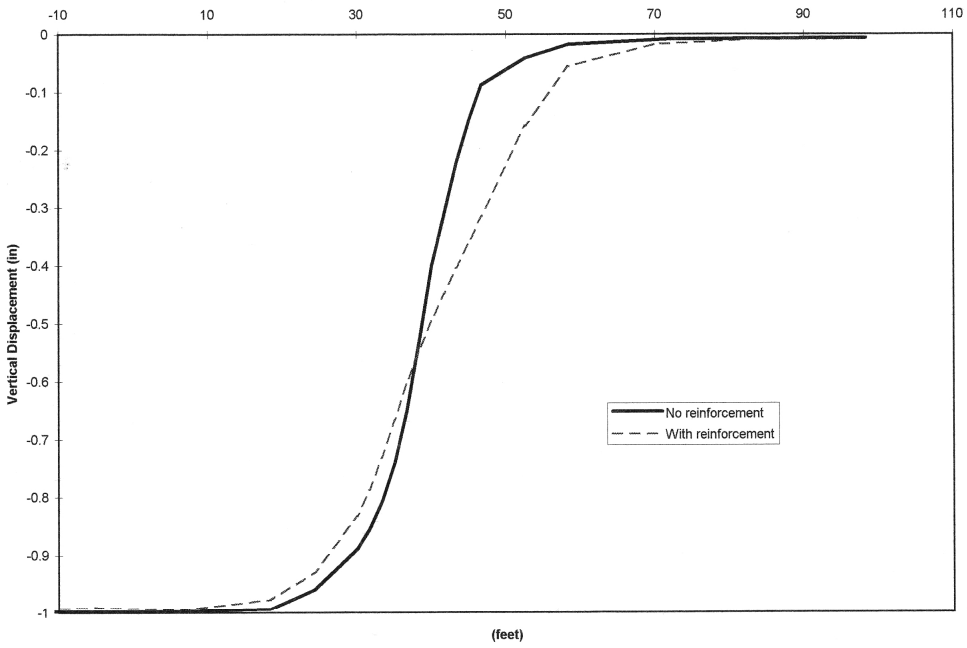

Figure 25 Finite element results showing beneficial effect of installing two layers of geogrids into compacted fill. The underlying differential fault offset is spread across a wider zone with reinforced fill, thereby reducing Hazards B and C. Case shown is for 6 m-high reinforced and unreinforced fill composed of Soil B for 2.8 cm of displacement across a normal fault dipping at 65 degrees (1.0 inch = 2.5 cm, and 1.0 feet = 0.305 m).

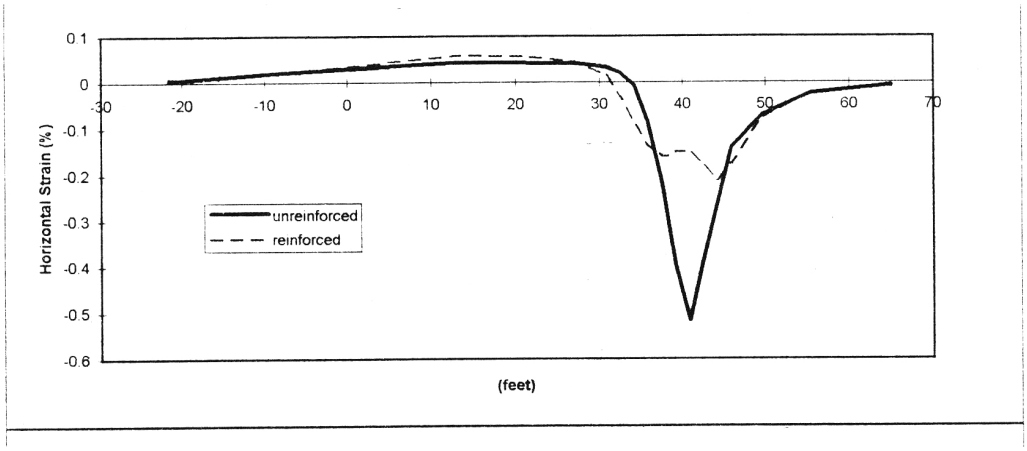

Figure 26 Reduction in horizontal tensile strains due to the use of geogrid reinforcement for same case described in Figure 25.

most critical soil case are shown in **Table 3**. As shown in **Figure 25**, the finite element results indicate that the geogrid reinforcement is effective in spreading the differential movement, across the distinct bedrock fault across a wider zone of general shear in the fill. Hence, the angular distortion across a reasonable width is reduced with the use of the geosynthetic reinforcement. In these plane strain analyses, the finite element boundary conditions impose uniform displacements at the left and right boundaries of the mesh, as one would expect if the underlying bedrock in this area displaced uniformly. The reinforced compacted fill increases the width of the transition zone at the ground surface.

For the controlling case (85^{o} dipping normal fault movement, Soil B), angular distortions were reduced from 1/260 to 1/330 for a 6 m-thick fill when two layers of geogrid with the baseline

properties were used. The use of reinforcement was relatively less effective, however, for shallower fill thickness such as 3 m, where the reduction in angular distortion was minimal. The use of reinforcement dramatically reduced the magnitude of tensile ground strains calculated near the ground surface for cases examined. Maximum tensile strains were typically reduced by at least half by installing two layers of geogrid as shown in **Figure 26**. Hence, reinforcement was useful in mitigating high tensile ground strains (Hazard C).

The finite element results indicate that if the height of fill is to be minimized to reduce the potentially deleterious effects of the other more routine design considerations (e.g. shrink/swell/collapse under static service loads, and vibration induced settlement under earthquake ground shaking), the use of reinforcement is desirable within the compacted fill placed over the bedrock faults exposed by grading in the hanging-wall bending moment normal fault area. A 7 m-high reinforced fill satisfied the project's preliminary performance criteria by "absorbing" the bedrock fault, limiting the angular distortion to 1/360, and limiting the tensile strain to less than 0.3% (**Table 3**).

6.5 Discussion and project recommendations

(1) *General*

The finite element results suggest that there are principally three geotechnical design techniques effective in mitigating the potential hazards associated with earthquake base rock fault rupture propagation through compacted fill. The hazards can be reduced by: (1) increasing the height of the compacted fill, (2) increasing the ductility of the compacted fill, and (3) installing soil-reinforcement within the compacted fill.

(2) *Use of compacted earth fill (reinforced and unreinforced)*

Laboratory test results indicated that the fill material response ranged from slightly brittle to ductile, depending on the soil type and relative compaction level. Ductility could be enhanced by placing the fill material wet of optimum at lower dry densities. The performance of the compacted fill could be further enhanced by increasing its thickness. The finite element results indicated that the proposed Restricted Use Zones (RUZ) delineated by setbacks for the active shallow thrust faults were adequate. In fact, a number of the setbacks could be brought in, making these restricted use zones narrower. The finite element results indicated that the hanging-wall bending moment normal faults that occurred throughout the project area would satisfy the project's preliminary performance criteria (Hazard B controlling with an angular distortion of 1/360) if they were covered by at least 9 m of in situ soil or unreinforced fill. Where this thickness of soil did not exist, the use of reinforced fill was explored

The benefits of using reinforced soil in this application was surmised from a review of physical model tests and conceptional elasto-plastic models recently published in the literature (e.g. Gray & Ohashi 1983, Jewell & Wroth 1987, Shewbridge & Sitar 1985, Shewbridge & Sitar 1989, Gray 1991, Shewbridge & Sitar 1991, Shewbridge & Sitar 1992). These publications indicate that in direct shear testing, sands reinforced with tensile reinforcement are less likely to form a distinct shear band, but instead, the reinforcement is effective in "spreading out" the imposed distinct boundary displacement. However, in less constrained torsional shear tests, reinforcement without appreciable bending resistance was less effective (Shewbridge 1987, Shewbridge & Sitar 1996), and both the direct shear tests and torsional shear testing were generally performed on soils with high relative densities (> 70%) at relatively low normal stresses, where the soil's volumetric response would be dilative. Reinforcement is effective in transforming a material with a strain softening response due to dilation along a distinct shear band into a strain hardening material with a higher failure strain (Shewbridge & Sitar 1992). Hence, reinforcement will be more effective when employed in dilative soils. Although the volumetric response of these partially saturated compacted soils during undrained shear is initially contractive, at higher strain levels, especially for the soils compacted to higher relative densities (i.e. R.C. > 95%), the soil response is primarily dilative.

Soil-reinforcement proved effective in spreading the differential movement across the bedrock fault across a wider zone of shear in the fill, thereby reducing the angular distortion (Hazard B), and horizontal tensile strains (Hazard C) at the ground surface. The height of the shear rupture zone in the compacted fill overlying the displaced bedrock fault (Hazard A) was effectively mitigated with the use of soil-reinforcement, but this hazard did not generally govern the design. The project's performance criteria could be achieved by installing 2 layers of geogrid within a 7 m-high compacted fill. The findings of this finite element study agree generally with the results of published laboratory tests which indicated that the geosynthetic reinforcement was effective in spreading differential movement in a direct shear apparatus across a wider zone of shear (e.g. Shewbridge & Sitar 1989).

(3) *Use of special foundations*

If satisfactory building performance is to be achieved at the project site using compacted fill heights less than 7 m, a combination of mitigation measures should be considered. One option involves the adjustment of the project's performance criteria that defines an acceptable level of ground deformation through the use of structural engineering mitigation measures. The tolerable criteria is intimately linked to the ductility and strength of the structure and its foundation and the manner in which the foundation is coupled to the ground. For example, the use of post-tensioned slabs in lieu of standard concrete foundation slabs allowed the angular distortion criterion to be increased from 1/480 to 1/360. If designed appropriately, a post-tensioned slab can withstand even greater levels of ground deformation. Modification of the project's performance criteria for houses should be based on the recommendations of a professional structural engineer familiar with foundation slab design. The foundation slabs should be designed to withstand the combined effects of angular distortion and tensile ground strain due to fault movement, as well as more routine design issues such as static fill deformation and seismically induced settlement.

As an example of the order of magnitude of ground deformation that may be acceptable for modern housing structures, Day (1990) performed surveys of damage to slab-on-grade one- and two-story housing structures that underwent differential settlement. The slabs-on-grade of the homes in the study group were generally 10 cm thick and reinforced with wire mesh, with exterior footings 30 cm wide by 45 cm deep and reinforced with steel rebar. These foundations are inferior to the thicker, post-tensioned slabs recommended for structures located in fault zones, however, the Day (1990) study provides insight, because it establishes a possible conservative criterion to be considered for this project.

Day (1990) found that cracking in the gypsum wall board panels is likely to occur if the angular distortion of the foundation (not the ground deformation) exceeds 1/300, and that structural damage of the wood columns and beams is likely to occur if the angular distortion of the foundation (again not the ground deformation) exceeds 1/100. Factors of safety should normally be applied to these values, so these observations suggest that if the slab can be designed to limit foundation deflection to less than about 1/200, structural damage should be avoided. Moreover, if the slab can limit foundation deflection to around 1/450, architectural damage is probably unlikely. On this project, consistent with the manner in which the Uniform Building Code addresses damage levels for the earthquake ground shaking hazard, functionality will be maintained if the foundation deflection is less than around 1/300. At this level of slab deflection, some dry wall cracking, etc. is possible, but it would be unlikely that housing components such as drywall were able to withstand the ground shaking associated with a near-source earthquake event without some damage, even without ground deformation resulting from fault rupture.

Slab reinforcement is one of the keys to mitigating the surficial hazards associated with fault rupture. Reinforced slabs performed significantly better than unreinforced slabs during the 1992 Landers earthquake. The proposed recommendations from the City of Los Angeles (1995) regarding increasing the level of reinforcement of residential slabs to minimize damage due to ground movements from seismic compaction is also consistent with this finding. In addition, it would be preferable if the slabs were underlain by polyethylene (plastic) sheets overlaying a clean granular soil-bedding layer. This limits the ground strain that can be transmitted to the foundation slab. Using a grade beam foundation system is another means of limiting the transfer of ground strain to the building foundation.

7. CONCLUSIONS

Surface fault rupture has been recognized as a principal earthquake hazard in the United States since the dramatic 1906 San Francisco earthquake on the San Andreas fault. Damage to houses from surface fault rupture during the 1971 San Fernando, California earthquake motivated the enactment of the Alquist-Priolo Act of 1972 in California, with the objective of avoiding the construction of homes across major active faults. Recently, major earthquakes producing significant surface fault rupture, such as the 1992 Landers, 1999 Kocaeli, 1999 Chi-Chi, and 1999 Duzce earthquakes, have reminded the profession and the public of the devastating effects of earthquake surface fault rupture on engineered structures and facilities. Some key observations from these recent events have been discussed with special emphasis on describing how ground movements associated with surface faulting affect structures.

Observations at recent earthquakes, such as the Landers, Kocaeli, and Chi-Chi earthquakes, have provided contrasting signals. On the one hand, avoidance of faults in the siting of structures has become more difficult because these observations show that the rupture zone can be much wider than

normally assumed, and rupturing can occur in previously unidentified zones. Conversely, the fact that simple structures located across major fault movements were able to survive ground fracturing, in terms of life safety (but not damage), suggests that we can design structures to withstand ground rupture.

Analytical procedures can be employed to evaluate the hazards associated with surface faulting and to develop reasonable mitigation measures. A project in Southern California where these procedures were applied was presented to illustrate the insight gained from sound engineering analysis of the problem. Similar to other forms of ground failure, such as mining subsidence and landslides, effective design strategies can be employed to address the hazards associated with surface faulting. These design measures include establishing non-arbitrary setbacks based on fault geometry, fault displacement, and the overlying soil; constructing earth fills, often reinforced with geosynthetics, to partially absorb and spread out the underlying ground movements; using slip layers to decouple ground movements from foundation elements; and designing strong, ductile foundation elements that can accommodate some level of deformation without compromising the functionality of the structure. It is hoped that these mitigation measures can used in future projects to rationally address the hazards associated with earthquake surface fault rupture.

ACKNOWLEDGMENTS: Partial support for the research efforts presented in this paper was provided by the David and Lucile Packard Foundation, and the National Science Foundation through Grant No. BCS-9157083. In addition, the Earthquake Engineering Research Institute and the Federal Emergency Management Agency provided financial support. Douglas Papay, the project engineer, and Mason Redding, the project engineering geologist, both of Pacific Materials Laboratory, Inc. of Camarillo, California are acknowledged for their efforts on the project described in this paper. I also wish to thank all those who have contributed in many ways over the years to my ongoing efforts to investigate the hazards associated with surface fault rupture, including my former students: A. Ashmawy, Johanna Fenton, Carlos Lazarte, Scott Merry, Diane Murbach, Adrian Rodriguez-Marek, and Patricia Thomas; my research partners: Jeff Bachuber, Aykut Barka, Lloyd Cluff, Ken Cruikshank, Turan Durgunoglu, Eldon Gath, G. Mukhopadhyay, Arvid Johnson, Keith Kelson, Bill Lettis, Bill Page, Tom Rockwell, and Raymond Seed. Mr. Rodolfo Sancio assisted me in the preparation of figures and Professor Kazuo Konagai's laboratory assistants put the paper into proper format for this workshop. Special recognition goes to my former thesis advisor, the later Professor H. Bolton Seed, who started me on the path of understanding the effects of earthquake fault rupture.

REFERENCES

Barka, A., and 18 others. [1999] "17 August 1999 Izmit earthquake, Northwestern Turkey [abs.]," *Eos, American Geophysical Union 1999 Fall Meeting*, **80:F647**.

Bonilla, M. G., and Lienkaemper, J. J. [1991] "Factors Affecting the Recognition of Faults in exploratory Trenches," *U. S. Geological Survey Bulletin*, **1947**, 54.

Bonilla, M. G. [1970] "Surface Faulting and Related Effects," in Earthquake Engineering, Weigel, R. L., ed., New Jersey, Prentice-Hall, 47-74.

Bonilla, M. G. [1988] "Minimum Earthquake Magnitude Associated with Coseismic Surface Faulting," *Bulletin of Assoc. of Engrg. Geologists*, **XXV(1)**, 17-29.

Boscardin, M. D. and Cording, E. J. [1989] "Building Response to Excavation-Induced Settlement," *Journal of Geotechnical Engineering*, ASCE, **115(1)**, 1-21.

Boulanger, R. W., J. D. Bray, S. H. Chew, R. B. Seed, J. M. Duncan and J. K. Mitchell [1991] "SSCOMPPC: A Finite Element Analysis Program for Evaluation of Soil-Structure Interaction, and Compaction Effects: PC Version 1.0," *Geotechnical Engineering Report*, Univ. of California, Berkeley, **UCB/GT/91-02**, 176.

Bray, Jonathan D. [1990] "The Effects of Tectonic Movements on Stresses and Deformations in Earth Embankments," *Dissertation Doctor of Philosophy*, University of California, Berkeley, 414.

Bray, J. D., R. B. Seed and H. B. Seed [1992] "On the Response of Earth Dams Subjected to Fault Rupture," *Proceedings of Stability and Performance of Slopes and Embankments - II*, 608-624.

Bray, J. D., A. Ashmawy, G. Mukhopadhyay and E. M. Gath [1993a] "Use of Geosynthetics to Mitigate Earthquake Fault Rupture Propagation Through Compacted Fill," *Proceedings of the Geosynthetics '93 Conference*, **1**, 379-392.

Bray, J. D., R. B. Seed and H. B. Seed [1993b] "1g Small-Scale Modelling of Saturated Cohesive Soils," *Geotechnical Testing Journal*, American Society for Testing and Materials, **16(1)**, 46-53.

Bray, J. D., R. B. Seed, L. S. Cluff and H. B. Seed [1994a] "Earthquake Fault Rupture Propagation through Soil," *Journal of Geotechnical Engineering*, ASCE, **120(3)**, 543-561.

Bray, J. D., R. B. Seed and H. B. Seed [1994b] "Analysis of Earthquake Fault Rupture Propagation through Cohesive Soil," *Journal of Geotechnical Engineering*, ASCE, **120(3)**, 562-580.

Chen, F. H. [1988] "Foundations on Expansive Soils," Elsevier Science Publishing Co., Inc., New York.

Chen, W.-S., and Y.-G. Chen [1999] "The characteristics of surface ruptures in association with 1999 Chichi earthquake in Taiwan [abs.]," *AGU 1999 Fall Meeting Program, Late Breaking Detailed Sessions*, **13**.

Chiu, J.-M., M. Ellis, P.A. Bodin, S. Pezeshk, and G. Patterson [1999] "Observations of rupture and damage from the 1999 Mw 7.6 Ji Ji (Taiwan) earthquake [abs.]," *AGU 1999 Fall Meeting Program, Late Breaking Detailed Sessions*, **14**.

Clough, G. W., and Duncan, J. M. [1969] "Finite Element Analyses of Port Allen and Old River Locks," *Geotechnical Engineering Report*, Univ. of California, Berkeley, **TE-69-3**.

Cole, D. A., Jr. and Lade, P.V. [1984] "Influence Zones in Alluvium Over Dip-Slip Faults," *Journal of Geotechnical Engineering*, ASCE, **110(5)**, 599-615.

Cundall, P. A. and Strack, O. D. L. [1979] "Discrete Numerical Model for Granular Assemblies," *Geotechnique*, **29(1)**, 47-65.

Day, R. W. [1990] "Differential Movement of Slab-On-Grade Structures," *Journal of Perf. Of Constructed Facilities*, ASCE, 4(4), 236-241.

Duncan, J. M., Byrne, P., Wong, K. S., and Mabry, P. [1980] "Strength, StressStrain and Bulk Modulus Parameters for Finite Element Analyses of Stresses and Movements in Soil Masses," *Geotechnical Engineering Report*, Univ. of California, Berkeley, **UCB/GT/80-01**.

Duncan, J.M., Seed, R. B. Wong, K.S., and Ozawa, Y. [1984] "FEADAM84: A Computer Program for Finite Element Analysis of Dams," *Research Report*, Department of Civil Engineering, Stanford Univ., **SU/GT/84-03**.

Duncan, J. M., and Lefebvre, G. A. M. [1973] "Earth Pressures on Structures Due to Fault Movement," *ASCE National Structural Engineering Meeting*.

Espinoza, R.D., Bray, J.D., Taylor, R.L., and Soga, K. [1995] "GeoFEAP: Geotechnical Finite Element Analysis Program," *Geotechnical Engineering Report*, Univ. of California, Berkeley, **UCB/GT/95-05(4)**, 500.

Fenton, Johanna S., and Bray, Jonathan D. [1994] "Relationship of Surficial Earth Materials to the Characteristics of the 1992 Landers Earthquake Surface Rupture," *Geotechnical Engineering Report*, Univ. of California, Berkeley, **UCB/GT/94-05**, 74.

Fumal, T.E., and 12 others. [1999] "Slip distribution and geometry of the Sakarya section of the 1999 Izmit earthquake ground rupture, Western Turkey [abs.]," *Eos, American Geophysical Union 1999 Fall Meeting*, **80:F669**.

Gray, D. H. [1991] "Deformation Characteristics of Reinforced Sand in Direct Shear," *Journal of Geotechnical Div.*, ASCE, **117(11)**, 1810-1812.

Gray, D. H. and Ohashi, H. [1983] "Mechanics of Fiber Reinforcements in Sand," *Journal of Geotechnical Div.*, ASCE, **109(3)**, 335-353.

Hart, E. W., W. A. Bryant, and J. A. Treiman [1993] "Surface faulting associated with the June 1992 Landers earthquake, California," *California Geology*, **46(1)**, 10-16.

International Conference of Building Officials [1997] "Uniform Building Code, Volume 2, Structural Engineering Design Provisions".

Jewell, R. A. and Wroth, C. P. [1987] "Direct Shear Tests on Reinforced Sand," *Geotechnique*, **37(1)**, 53-68.

Johnson, Arvid M., Fleming, Robert W., and Cruikshank, Kenneth M. [1993] "Broad Belts of Shear Zones as the Common Form of Surface Rupture Produced by the 28 June 1992 Landers, California, Earthquake," *U. S. G. S. Open-File Report*, **93-348**, 48.

Ke, T-C. and Bray, J. D. [1995] "Modeling of Particulate Media Using Discontinuous Deformation Analysis," *Journal of Engineering Mechanics*, ASCE, **121(11)**, 1234-1243.

Kelson, K. and 13 other authors [2001] "Fault-related surface deformation resulting from the Chi-Chi (Taiwan) earthquake," *Earthquake Spectra Journal*, Special Volume on the Chi-Chi Taiwan Earthquake of September 21, 1999 Reconnaissance Report, in press.

Kratzsch, H. [1983] "Mining Subsidence Engineering, Springer Verlag," Berlin, 543.

Lade, P. V. and Cole, D. A., Jr. [1984] "Influence Zones in Alluvium Over Dip-Slip Faults," *Journal of Geotechnical Engineering*, ASCE, **110(5)**, 599-615.

Lazarte, C. A. [1996] "The Response of Earth Structures to Surface Fault Rupture," Ph.D. Thesis, Department of Civil Engineering, Univ. of California, Berkeley.

Lazarte, C. A, J. D. Bray, A. M. Johnson and R. E. Lemmer [1994] "Surface Breakage of the 1992 Landers Earthquake and Its Effects on Structures," *Bulletin of the Seismological Society of America*, **84(3)**, 547-561.

Lazarte, C.A. and Bray, J.D. [1995] "Observed Surface Breakage due to Strike-Slip Faulting," *Third International Conference on Recent Advances in Geotechnical Engineering and Soil Dynamics*, **II**, 635-640.

Lazarte, C.A. and Bray, J.D. [1996] "A Study of Strike-Slip Faulting Using Small-Scale Models," *Geotechnical Testing Journal*, American Society for Testing and Materials, **19(2)**, 118-129.

Lee, C.-T., K.I. Kelson, and K.-H. Kang [2000] "Hangingwall deformation and its effects on buildings and structures as learned from the Chelungpu faulting in the 1999 Chi-Chi, Taiwan earthquake," *Proceedings of International Workshop on Annual Commemoration of the Chi-Chi Earthquake*.

Lettis, W. and 21 other authors [2000] "Surface Fault Rupture," *Earthquake Spectra Journal*, Chapter 2 in the Special Volume on the Turkey Earthquake of August 17, 1999 Reconnaissance Report, 11-52.

Ma, K.-F., C.-T. Lee, Y.-B. Tsai, and T.-C. Shin [1999] "The Chi-Chi, Taiwan earthquake: Large surface displacements on an inland thrust fault," *EOS Transactions*, AGU, **80:605**.

Mitchell, J.K. [1976] "Fundamentals of Soil Behavior," John Wiley, New York, 437.

Murbach, D. [1994] "Characteristics of the 1992 Fault Rupture Adjacent to Distressed Structures, Landers, California," *The 1994 NEHRP Professional Fellowship Report, Project Research Advisors: Dr. Jonathan D. Bray and Dr. Thomas K. Rockwell*, Earthquake Engineering Research Institute, 73.

Simo, J. C., Armero, F. and Taylor R. L. [1993] "Improved versions of assumed enhanced strain tri-linear elements for 3-D finite deformation problems," *Comp. Methods in App. Mech. & Engrg.*, **110**, 354-386.

Sherard, J. L., Cluff, L. S., and Allen, C. R. [1974] "Potentially active faults in dam foundations," *Geotechnique*, **24**, 367-427.

Shewbridge, S. E., and Sitar, N. [1985] "The Influence of Fiber Properties on the Deformation Characteristics of Fiber-Soil Composites," *Geotechnical Engineering Report*, Univ. of California, Berkeley, **UCB/GT/85-02**.

Shewbridge, S. E. [1987] "The Influence of Reinforcement Properties on the Strength and Deformation Characteristics of a Reinforced Sand," Ph. D. Thesis, Univ. of California, Berkeley.

Shewbridge, S. E., and Sitar, N. [1989] "Deformation Characteristics of Reinforced Sand in Direct Shear," *Journal of Geotechnical Engineering*, ASCE, **115(8)**, 1134-1147.

Shewbridge, S. E., and Sitar, N. [1990] "Deformation-Based Model for Reinforced Sand," *Journal of Geotechnical Engineering*, ASCE, **116(7)**, 1153-1170.

Shewbridge, S. E., and Sitar, N. [1991] "Closure to Deformation Characteristics of Reinforced Sand in Direct Shear," *Journal of Geotechnical Engineering*, ASCE, **117(8)**, 1812-1817.

Shewbridge, S. E., and Sitar, N. [1992] "Shear Zone Formation and Slope Stability Analysis," Geotech. Spec. Pub. No. 31, ASCE Spec. Conf. Stab. and Perf. of Slopes and Embankments II, ASCE, 358-370.

Shewbridge, S. E., and Sitar, N. [1996] "Formation of Shear Zones in Reinforced Sand," *Journal of Geotechnical Engineering*, ASCE, **122(11)**, 873-885.

Shi, G.-H. and Goodman, R. E. [1989] "Generalization of Two-Dimensional Discontinuous Deformation Analysis for Forward Modeling," *Int. Jour. for Num. and Anal. Methods in Geomech.*, **13(4)**, 359-380.

Thomas, P.J. and Bray, J.D. [1999] "Capturing the Nonspherical Shape of Granular Media with Disk Clusters," *Journal of Geotechnical and Geoenvironmental Engineering*, ASCE, **125(3)**.

Wahls, H. E. [1994] "Tolerable Deformations," *Proceedings of Settlement' 94*, ASCE, Geotechnical Special Publication.

Whittaker, B. N., and Reddish, D. J. [1989] "Subsidence: Occurrence, Prediction and Control," Elsevier, Science Publishing Co., Inc., New York.

Zienkiewicz, O. C. and Taylor, R. L. [1991] "The Finite Element Method," John Wiley & Sons, New York.

(Received December 15, 2000)